Journal of Molecular Science
Volume 35 Issue 2, Year of Publication 2025, Page 269-279
DoI-17.4687/1000-9035.2025.037

Journal of Molecular Science

Journal of Molecular Science
www.jmolecularsci.com ISSN:1000-9035

WES of MDR *Acinetobacter baumannii* SO_1077_3 through Illumina and Nanopore

Janakiram Bobbillapati[1], Monika Ranjan Tatapudi[2], J. Naveena Lavanya Latha*[3] AS Smiline Girija[1*]
[1]Department of Microbiology, Saveetha dental college, Saveetha university, Chennai.
[2]Department of Child health nursing, KSR college of nursing, Guntur, A.P.
[*3]Department of Biotechnology, Krishna University, Machilipatnam, Andhra Pradesh.

Email: smilinejames25@gmail.com

Article Information
Received: 20-06-2025
Revised: 07-07-2025
Accepted: 25-07-2025
Published: 11-08-2025

Keywords
WES of MDR Acinetobacter baumannii

ABSTRACT

Acinetobacter baumannii is a gram-negative bacterium known for causing infections primarily in hospital settings. It has the potential to rapidly develop resistance to multiple drugs (MDR), extended drugs (XDR), and even all available drugs (PDR). Despite extensive research, a full understanding of its antibiotic resistance mechanisms and the virulence factors driving its pathogenicity remains incomplete. This study analyzed the drug resistance profile and genomic characteristics of a PDR A. baumannii strain, SO_10770_3, isolated from an endotracheal aspirate. The results indicated that the SO_10770_3 strain was resistant to all tested antibiotics. Through de novo genome assembly, the total genome size was determined to be 3,924,675 base pairs. Gene Ontology (GO) analysis classified 10,915 genes into 45 categories, while 1,687 genes were linked to 34 pathways in the Kyoto Encyclopedia of Genes and Genomes (KEGG). Clusters of Orthologous Genes (COG) annotation revealed 3,189 genes in the strain. Additionally, 59 virulence factors were identified using the Virulence Factors of Pathogenic Bacteria Database (VFDB). Antibiotic resistance genes for aminoglycosides, β-lactams, erythromycin, and streptogramins were found through the Comprehensive Antibiotic Resistance Database (CARD). The study also identified resistance-nodulation-cell division (RND) and major facilitator superfamily (MFS) transporters associated with drug efflux. Overall, this research provided a detailed genomic analysis of strain SO_10770_3, exploring its antibiotic resistance and potential virulence factors through GO, COG, and KEGG analyses.

INTRODUCTION:

Acinetobacter baumannii is a gram-negative, opportunistic coccobacillus commonly associated with hospital-acquired infections such as bloodstream infections, pneumonia, meningitis, and urinary tract infections (Munoz-Price, Weinstein, 2008; Peleg et al., 2008; Antunes et al., 2014). It is particularly prevalent in intensive care units (ICUs) and has become a leading cause of healthcare-associated outbreaks worldwide. The Infectious Diseases Society of America (IDSA) has ranked A. baumannii as one of the top six priority pathogens due to its high level of threat (Peterson, 2009).

The rise of multidrug-resistant (MDR) A. baumannii presents a significant public health concern. Studies have noted the increasing presence of MDR bacterial pathogens in humans, animals, and even aquatic species, underscoring the importance of regular antimicrobial susceptibility testing to determine effective treatments and identify MDR strains (Algammal et al., 2020a; Algammal et al., 2020b; Abolghait, 2020; Makharita et al., 2020; Algammal et al., 2021). MDR A. baumannii is resistant to various antibiotics, including β-lactams, fluoroquinolones, tetracyclines, and aminoglycosides (Nikaido, 2009). This resistance is often linked to the presence of resistance-nodulation-division (RND) transporters and outer membrane proteins, which help the bacteria expel drugs from their cells (Abdi et al., 2020 and Zhang et al., 2021).

As treatment options for MDR A. baumannii become more restricted, colistin and tigecycline remain the last effective antibiotics. However, the bacterium can also become extensively drug-resistant (XDR), showing resistance to all antibiotics except colistin and tigecycline, leading to severe healthcare-associated infections (Kyriakidis et al., 2021; Mulani et al., 2019; Kengkla et al., 2018; Liu et al., 2021). Recently, pan-drug-resistant (PDR) strains of A. baumannii, which are resistant to both colistin and tigecycline, have been identified, further reducing treatment options and increasing mortality rates (Cai et al., 2012; O'Hara et al., 2013).

Several virulence factors contribute to the pathogenicity of A. baumannii, including pili, outer membrane porins, phospholipases, proteases, lipopolysaccharides, capsular polysaccharides, protein secretion systems, and iron-chelating systems. Some strains possess genes that enable them to adhere, invade, survive, and form biofilms on surfaces, increasing their virulence (Gentilini et al., 2018).

Given the increasing prevalence of infections and the limited availability of effective antibiotics, A. baumannii is a highly successful pathogen in healthcare settings. To combat this issue, it is critical to better understand the mechanisms behind its antibiotic resistance and the virulence factors that contribute to its pathogenicity.

The advent of whole-genome sequencing technology has greatly advanced the study of bacterial genomes, enabling deeper insights into the mechanisms of antibiotic resistance and pathogenesis in A. baumannii (Jalal et al., 2021; Naha et al., 2021). Despite this progress, there is still a lack of data on colistin-resistant A. baumannii strains isolated from India. To address this, we performed a whole-genome characterization of the PDR-A. baumannii strain SO_10770_3 using de novo assembly with Illumina technology. Gene prediction and functional annotation were carried out using publicly available databases. The aim of this analysis was to identify potential antibiotic-resistant genes and virulence factors in this strain, which could help clarify the mechanisms behind A. baumannii's resistance and provide a basis for future clinical management and treatment strategies.

2. MATERIALS AND METHODS:

2.1 Isolation and Identification of Acinetobacter baumannii:

In this research, a multidrug-resistant (MDR) strain of Acinetobacter baumannii, labeled SO_10770_3, was isolated from the blood sample of a patient suffering from ventilator-associated pneumonia, along with cardiac and respiratory failure, in 2023 at the Critical Care Unit of NRI Medical College, Andhra Pradesh, India. The strain was cultured using 5% sheep blood agar, chocolate agar, and MacConkey agar, all commercially obtained from HI Media, India. The cultures were incubated at 35°C for 18–24 hours. The bacterial strain was then identified through 16S rRNA sequencing using the Sanger method.

2.2 Antimicrobial Susceptibility Testing:

Antimicrobial susceptibility testing was performed using a Vitek 2 GN ID Test Kit and Vitek 2 AST 407 Critical Care Kit on the BioMerieux Vitek 2 Automated Microbiology System (France), following the manufacturer's instructions. Minimum inhibitory concentration (MIC) breakpoints were determined according to the Clinical and Laboratory Standards Institute (CLSI) guidelines (M100, 27th edition). Antibiotics tested included Ticarcillin/Clavulanic acid, ceftazidime, doripenem, cefepime, imipenem, meropenem, Cefoperazone/Sulbactam, ciprofloxacin, levofloxacin, gentamicin, piperacillin/tazobactam, trimethoprim/sulfamethoxazole, tigecycline, minocycline, and colistin. Control strains used were Escherichia coli ATCC 25922 and Pseudomonas aeruginosa ATCC 27853 as recommended by CLSI.

2.3 DNA Quality Control:

Genomic DNA was extracted from the bacterial lysate using the Qiagen DNeasy Blood and Tissue Kit (Cat. No. 69506). For each sample, 100 µL of AL buffer and 20 µL of Proteinase K were added, followed by a 2-hour incubation at 56°C. RNase A treatment (MP Biomedicals, Cat. No. 2101076) was performed for 20 minutes at 65°C. After the addition of 200 µL of ethanol, the sample was loaded into a spin column and centrifuged at 8000 rpm, discarding the flow-through. The wash steps were completed according to the manufacturer's instructions. DNA was eluted in 10 mM Tris-HCl buffer, pH 8.0 (Cat. No. T3038-1L). The DNA's purity and concentration were evaluated using a Nanodrop spectrophotometer (Thermo Scientific 2000) and a Qubit dsDNA HS Assay Kit (Q32854). DNA integrity was verified through agarose gel electrophoresis. Samples that met quality standards were prepared for Illumina and Nanopore sequencing.

2.4 Strain Purity Check:

To confirm strain purity, the 16S rRNA gene was amplified via PCR using 30-50 ng of genomic DNA as a template. The reaction mix included 16S rDNA primers (27F and 1492R) and Takara ExTaq polymerase in a 25 µL reaction. The 1.5 kb PCR product was purified and used for Sanger sequencing. BLAST analysis revealed that strain SO_10770_3 was identified as Acinetobacter baumannii with 99.28% identity.

2.5 Illumina Library Preparation:

Library construction was performed at Genotypic Technology using the QIA Seq FX DNA Library Preparation protocol (Cat. No. 180475), following the manufacturer's guidelines. In brief, 50 ng of DNA, quantified by Qubit, underwent enzymatic fragmentation, end-repair, and A-tailing in a single reaction tube using the FX Enzyme Mix from the QIA Seq FX DNA kit. Index-incorporated Illumina adapters were ligated to the fragments, forming the sequencing library. Six cycles of indexing-PCR were conducted to enrich the adapter-tagged fragments, followed by purification using JetSeq Beads (Bio, #68031). The final libraries were quantified with a Qubit fluorometer, and the fragment size distribution was assessed using the Agilent 2200 TapeStation. The library showed an average fragment size of 387 bp and sufficient concentration for sequencing.

2.6 Illumina Sequencing:

The libraries were sequenced on the Illumina NovaSeq 6000 (San Diego, USA) using 150 bp paired-end chemistry. The sequencing run was de-multiplexed using Bcl2fastq v2.20 software, generating FastQ files based on unique dual barcode sequences. Quality assessment of the sequencing data was done using FastQC v0.11.8. Adapter sequences were removed, and only bases with a quality score above Q30 were kept, with low-quality bases filtered out before downstream analysis.

2.7 Nanopore Library Preparation and Sequencing:

A total of 600 ng of purified genomic DNA was end-repaired using the NEBNext Ultra II End Repair Kit (New England Biolabs, USA) and cleaned with 1x AMPure beads (Beckman Coulter, USA). Barcode ligation was performed using the NEB Blunt/TA Ligase (New England Biolabs, USA) with the EXP-NBD104 kit (Oxford Nanopore Technologies). The barcoded DNA was ligated with adapters using the NEBNext Quick Ligation Module (New England Biolabs, USA) for 15 minutes and purified using 0.6x AMPure beads. The final sequencing library was eluted in 15 µL of elution buffer. Sequencing was carried out on the GridION X5 platform (Oxford Nanopore Technologies, UK) with a Spot ON flow cell (FLO-MIN106) over a 48-hour protocol. The raw reads in 'fast5' format were base-called and converted to 'fastq5' format using Guppy v2.3.4, and demultiplexed for further analysis.

3.0 RESULTS

3.1.1 Bacterial Isolation, Identification, and Antimicrobial Susceptibility Testing:

The Acinetobacter baumannii strain SO_10770_3 was isolated from the endotracheal aspirate of a patient admitted to NRI General Hospital. On blood and chocolate agar, the colonies appeared smooth, raised, and opaque, while on MacConkey agar, they formed non-lactose fermenting colonies. The antimicrobial susceptibility testing revealed that the strain was resistant to all tested antibiotics, as detailed in Table 4.

3.1.2 Data Analysis:

For the A. baumannii strain SO_10770_3, approximately 2.8 million paired-end sequencing reads were generated using Illumina technology. In addition, around 0.83 GB of Nanopore long-read data was obtained for two bacterial samples. The Illumina reads were processed using Trimgalore v0.4.0 to remove adapters and filter out low-quality reads. The Nanopore reads were filtered for a minimum quality score of 10 using Nanofilt-v2.8.0, with adapter trimming carried out using Porechop-v0.2.3. A hybrid genome assembly of both short and long reads was performed using Unicycler-v0.4.8, an assembly tool that integrates both data types. The draft genome, approximately 4 Mb in size, was obtained with three contigs for each sample.

Gene and protein prediction was conducted using the Prokka-v1.14 tool, identifying 3,844 proteins in SO_10770_3. Further annotation of these predicted proteins was performed using the DIAMOND BlastP program, which compared them against the Uniprot Bacterial database with a minimum identity cutoff of 30%. This allowed for the assignment of functional and gene ontology information. Pathway analysis was conducted using the KAAS database, with five Acinetobacter species serving as references.

To further analyze the assembled genomes, DNA-DNA hybridization was performed using the TYGS server, and average nucleotide identity (ANI) was calculated using the ANI Calculator (Kotas Lab). Comparative genome analysis of the bacterial sample against the closest reference strain was conducted using the BRIGv0.95 tool. Antibiotic resistance genes were identified using the Comprehensive Antibiotic Resistance Database (CARD), while virulence genes were identified using the Virulence Factors Database (VFDB). Genes with a minimum identity of 70% and query coverage were selected as the best hits. Additionally, mobile genetic elements were identified using the ACLAME database within 500 base pairs upstream and downstream of the antimicrobial resistance (AMR) and virulence factor genes. Figure 5 below illustrates the complete bioinformatics workflow.

3.1.3 Primary Analysis:

Illumina sequencing for the SO_10770_3 strain produced approximately 2.8 million reads, while Nanopore sequencing generated 0.83 GB of long-read data. The Illumina reads were processed using Trimgalore, where adapters were trimmed, and low-quality reads (those with a quality score below 30 or shorter than 20 base pairs) were removed. Similarly, the Nanopore long reads were filtered for quality (score below 10) and had their adapters trimmed using Porechop. The read statistics are summarized in Tables 4 and 5.

3.2 Secondary Analysis:

3.2.1 De Novo Hybrid Assembly:

The hybrid genome assembly for the bacterial sample was performed using both Illumina short-read and Nanopore long-read data in the Unicycler assembler. The resulting draft genome contained three contigs with a total size of approximately 4 Mb for both bacterial samples. Validation of the assembly was carried out using the NCBI NR Blast program, which used a ~200 Kb input sequence from the longest contig. The results indicated strong homology with reference Acinetobacter species. The two smaller contigs were identified as plasmids based on the BLAST results. The Illumina reads were mapped back to the assembled draft genome, showing high read utilization, with approximately 97.9% of reads mapped for sample SO_10770_3. The assembly statistics are presented in Table 6, with BLAST results illustrated in Figures 6a to 6c.

3.2.2 Gene Prediction and Gene Ontology Annotation

Gene and protein predictions for SO_10770_3 were performed using the Prokka tool on the draft genome, identifying a total of 3,844 predicted proteins. Gene Ontology (GO) annotation was conducted using the DIAMOND Blast program against the UniProt Bacterial database, applying a minimum identity cutoff of 30% to identify the best hits. Out of 3,844 proteins, 3,842 were successfully annotated. The GO annotation results are depicted in Figure 7.

3.2.3 Pathway Analysis:

Pathway analysis for SO_10770_3 was conducted using the KAAS database. The protein sequences served as input for metabolic pathway analysis, with functional annotations derived from BLAST comparisons against the manually curated KEGG GENES database. The output included KO (KEGG Orthology) assignments and KEGG pathway maps. The top 10 pathway entries are shown in Figure 8.

3.2.4 DNA-DNA Hybridization Analysis:

DNA-DNA hybridization analysis was performed on the assembled draft genome using the Type Strain Genome Server (TYGS). This tool provides taxonomic classification within bacterial datasets and generates genome-scale phylogenies with support values and indicators of tree reliability. The resulting phylogenetic analysis revealed that the draft genome of SO_10770_3 was closely related to Acinetobacter baumannii ATCC19606, with an average sequence identity (d4) of 81.5%. The phylogenetic tree is shown in Figure 9.

3.2.5 Average Nucleotide Identity (ANI):

ANI analysis for the assembled genome of SO_10770_3 was carried out using the ANI Calculator, comparing it against the reference genome of Acinetobacter baumannii ATCC19606. Using default parameters (e.g., minimum length of 700 bp, minimum identity of 70%), the mean identity for SO_10770_3 was determined to be 97.91%. The ANI results are presented in Figure 10.

3.2.6 Comparative Genome Analysis:

A comparative genome analysis was performed on the draft genome of SO_10770_3 using the BRIG tool. This tool generated a circular genome comparison between SO_10770_3 and the reference genome of Acinetobacter baumannii ATCC19606. The output displays the similarity between the central reference sequence and other sequences in concentric rings, with BLAST matches color-coded according to percentage identity. The circular genome plot is provided in Figure 11.

3.2.7 Antimicrobial Resistance (AMR) and Mobile Genetic Elements (MGE) Analysis:

Antimicrobial resistance (AMR) genes in the draft genome of SO_10770_3 were identified using a homology-based approach (BLASTX) against the CARD database. The analysis was filtered for high-confidence results, retaining hits with at least 70% identity and query coverage. A total of 395 AMR-related hits were found, representing several gene families such as resistance-nodulation-cell division (RND) efflux pumps, rifamycin-resistant RNA polymerase subunits, fluoroquinolone-resistant gyrA, and more. These genes confer resistance to various antibiotics including cephalosporins, macrolides, fluoroquinolones, carbapenems, and tetracyclines. To assess the potential for horizontal gene transfer, 500 bp upstream and downstream regions of the AMR genes were examined for mobile genetic elements (MGEs) using BLASTX against the ACLAME database. For SO_10770_3, 55 MGE hits were identified upstream and 165 downstream of AMR genes, indicating a potential risk of horizontal gene transfer.

3.2.8 Virulence Factors (VF) and Mobile Genetic Elements (MGE) Analysis:

Virulence factor (VF) genes in the draft genome of SO_10770_3 were identified through a homology-based approach (BLASTX) against the VFDB. Hits with at least 70% identity and query coverage were retained, resulting in 341 virulence-associated proteins being identified. These proteins were associated with functions such as biofilm formation, efflux pumps, capsular polysaccharide biosynthesis, and iron acquisition systems. For the mobile genetic elements analysis, the regions 500 bp upstream and downstream of the VF genes were examined using BLASTX against the ACLAME database. Only one MGE hit was identified upstream of the VF genes, while no MGEs were found downstream, suggesting a limited risk of horizontal gene transfer for virulence factors in SO_10770_3.

4. DISCUSSION:

Whole genome sequencing of bacterial samples was conducted using both Illumina and Nanopore technologies to assemble and annotate the bacterial genome. For sample SO_10770_3, Illumina sequencing produced approximately 2.8 million reads, with sequencing coverage between 175X and 211X. Nanopore sequencing generated around 0.83 GB of long-read data, achieving coverage of approximately 228X. The genome size was estimated to be about 4 MB using the K-mer method through the Kmergenie tool, with an optimal K-mer value of 57 for SO_10770_3. A de novo hybrid assembly resulted in a draft genome of approximately 4 MB, with a GC content of 39%. Gene prediction from the draft genome identified 3,844 proteins, the majority of which (around 99%) were successfully annotated and further analyzed for functional roles and pathways. DNA-DNA hybridization analysis revealed that the bacterial sample was closely related to Acinetobacter baumannii ATCC19606, with an average nucleotide identity (ANI) of 97.91% for SO_10770_3 compared to the reference strain. The study also identified 395 antimicrobial resistance (AMR) genes with at least 70% identity and significant protein coverage, alongside 55 mobile genetic elements (MGEs) upstream and 165 MGEs downstream of these AMR genes, indicating potential horizontal gene transfer. Additionally, 341 virulence genes were detected, with only one MGE found upstream, suggesting a lower risk of horizontal gene transfer for these virulence genes. A circular genome comparison between the SO_10770_3 draft genome and the Acinetobacter baumannii ATCC19606 reference strain showed nearly 100% identity.

In conclusion, this study identified and characterized the Multi Drug Resistant strain of A. baumannii strain SO_10770_3 from an endotracheal aspirate of a patient in the critical care unit at NRI Medical College, Andhra Pradesh, India, in 2023. Knowledge of this bacterial pathogen at the genomic level has not been reported previously from India. We reported and updated the new A. baumannii strain SO_10770_3 in the NCBI Database and characterized the SO_10770_1 in the genomic level data, i.e. GO, COG, and KEGG. The antibiotic resistance genotype and phenotype as well as the presence of potential virulence associated factors were investigated.

5. REFERENCES:

1. Antunes LC, Visca P, Towner KJ. Acinetobacter baumannii: evolution of a global pathogen. Pathog Dis. 2014;71(3):292–301.
2. Munoz-Price LS, Weinstein RA. Acinetobacter infection. N Engl J Med. 2008;358(12):1271–1281.
3. Peleg AY, Seifert H, Paterson DL. Acinetobacter baumannii: emergence of a successful pathogen. Clin Microbiol Rev. 2008;21(3):538–582.
4. Peterson LR. Bad bugs, no drugs: no ESCAPE revisited. Clin Infect Dis. 2009;49(6):992–993.
5. Algammal AM, El-Kholy AW, Riad EM, Mohamed HE, Elhaig MM, Yousef SAA, et al. Genes encoding the virulence and the antimicrobial resistance in enterotoxigenic and shiga-toxigenic E. coli isolated from diarrheic calves. Toxins (Basel). 2020;12(6).
6. Algammal AM, El-Sayed ME, Youssef FM, Saad SA, Elhaig MM, Batiha GE, et al. Prevalence, the antibiogram and the frequency of virulence genes of the most predominant bacterial pathogens incriminated in calf pneumonia. AMB Express. 2020;10(1):99.
7. Abolghait SK, Fathi AG, Youssef FM, Algammal AM. Methicillin-resistant Staphylococcus aureus (MRSA) isolated from chicken meat and giblets often produces staphylococcal enterotoxin B (SEB) in non-refrigerated raw chicken livers. Int J Food Microbiol. 2020;328:108669.
8. Algammal AM, Hashem HR, Al-Otaibi AS, Alfifi KJ, El-Dawody EM, Mahrous E, et al. Emerging MDR-

Mycobacterium avium subsp. avium in house-reared domestic birds as the first report in Egypt. BMC Microbiol. 2021;21(1):237.

9. Makharita RR, El-Kholy I, Hetta HF, Abdelaziz MH, Hagagy FI, Ahmed AA, et al. Antibiogram and genetic characterization of carbapenem-resistant gram-negative Pathogens Incriminated in Healthcare-Associated Infections. Infect Drug Resist. 2020;13:3991–4002.
10. Nikaido H. Multidrug resistance in bacteria. Annu Rev Biochem. 2009;78:119–146.
11. Abdi SN, Ghotaslou R, Ganbarov K, Mobed A, Tanomand A, Yousefi M, et al. Acinetobacter baumannii efflux pumps and antibiotic resistance. Infect Drug Resist. 2020;13:423–434.
12. Zhang Y, Fan B, Luo Y, Tao Z, Nie Y, Wang Y, et al. Comparative analysis of carbapenemases, RND family efflux pumps and biofilm formation potential among Acinetobacter baumannii strains with different carbapenem susceptibility. BMC Infect Dis. 2021;21(1):841.
13. Kyriakidis I, Vasileiou E, Pana ZD, Tragiannidis A. Acinetobacter baumannii antibiotic resistance mechanisms. Pathogens. 2021;10(3).
14. Mulani MS, Kamble EE, Kumkar SN, Tawre MS, Pardesi KR. Emerging strategies to combat ESKAPE pathogens in the Era of antimicrobial resistance: A Review. Front Microbiol. 2019;10:539.
15. Kengkla K, Kongpakwattana K, Saokaew S, Apisarnthanarak A, Chaiyakunapruk N. Comparative efficacy and safety of treatment options for MDR and XDR Acinetobacter baumannii infections: a systematic review and network meta-analysis. J Antimicrob Chemother. 2018;73(1):22–32.
16. Liu J, Shu Y, Zhu F, Feng B, Zhang Z, Liu L, et al. Comparative efficacy and safety of combination therapy with high-dose sulbactam or colistin with additional antibacterial agents for multiple drug-resistant and extensively drug-resistant Acinetobacter baumannii infections: A systematic review and network meta-analysis. J Glob Antimicrob Resist. 2021;24:136–147.
17. O’Hara JA, Ambe LA, Casella LG, Townsend BM, Pelletier MR, Ernst RK, et al. Activities of vancomycin-containing regimens against colistin-resistant Acinetobacter baumannii clinical strains. Antimicrob Agents Chemother. 2013;57(5):2103–2108.
18. Cai Y, Chai D, Wang R, Liang B, Bai N. Colistin resistance of Acinetobacter baumannii: clinical reports, mechanisms and antimicrobial strategies. J Antimicrob Chemother. 2012;67(7):1607–1615.
19. Gentilini F, Turba ME, Pasquali F, Mion D, Romagnoli N, Zambon E, et al. Hospitalized pets as a source of carbapenem-resistance. Front Microbiol. 2018;9:2872.
20. Jalal D, Elzayat MG, Diab AA, El-Shqanqery HE, Samir O, Bakry U, et al. Deciphering multidrug-resistant Acinetobacter baumannii from a pediatric cancer hospital in Egypt. mSphere. 2021:e0072521.
21. Naha A, Vijayakumar S, Lal B, Shankar BA, Chandran S, Ramaiah S, et al. Genome sequencing and molecular characterisation of XDR Acinetobacter baumannii reveal complexities in resistance: Novel combination of sulbactam-durlobactam holds promise for therapeutic intervention. J Cell Biochem. 2021.
22. Hoff, Katharina & Stanke, Mario. (2018). Predicting Genes in Single Genomes with AUGUSTUS. Current Protocols in Bioinformatics. 65. 10.1002/cpbi.57.
23. Wick RR, Judd LM, Holt KE. Performance of neural network base calling tools for Oxford Nanopore sequencing. Genome biology. 2019 Dec; 20:1-0.
24. Hesse, Uljana. (2023). K-Mer-Based Genome Size Estimation in Theory and Practice. Methods in molecular biology (Clifton, N.J.). 2672. 79-113. 10.1007/978-1-0716-3226-0_4.
25. Wick RR, Judd LM, Gorrie CL, Holt KE. Unicycler: resolving bacterial genome assemblies from short and long sequencing reads. PLoS computational biology. 2017 Jun 8;13 (6) :e1005595.
26. Cho JC, Tiedje JM. Bacterial species determination from DNA-DNA hybridization by using genome fragments and DNA microarrays. Appl Environ Microbiol. 2001 67 (8):3677-82. doi: 10.1128/AEM.67.8.3677-3682.2001.
27. Hyun, J.C., Monk, J.M., Szubin, R. et al. Global pathogenomic analysis identifies known and candidate genetic antimicrobial resistance determinants in twelve species. Nat Commun 14, 7690 (2023). https://doi.org/10.1038/s41467-023-43549-9
28. D'Onofrio V, Cartuyvels R, Messiaen PEA, Barišić I, Gyssens IC. Virulence Factor Genes in Invasive Escherichia coli Are Associated with Clinical Outcomes and Disease Severity in Patients with Sepsis: A Prospective Observational Cohort Study. Microorganisms. 2023 Jul 17;11(7):1827. doi: 10.3390/microorganisms11071827.
29. Kondo K, Kawano M, Sugai M.2021.Distribution of Antimicrobial Resistance and Virulence Genes within the Prophage-Associated Regions in Nosocomial Pathogens. mSphere6: 10.1128/msphere.00452-21.https://doi.org/10.1128/msphere.00452-21

Table 1: Estimated DNA Concentration and Purity

S.No	**Sample ID**	**Nanodrop QC**				**Qubit QC**		
		ng/ul	260/280	260/230	Yield (ng)	Qubit conc.	Vol (ul)	Yield (ng)
1	SO_10770_3	60.9	1.91	1.53	1096.2	52.4	17	890.8

Table 2: Description of libraries

Sl.No	**Sample ID**	**Qubit Conc. (ng/ul)**	**Vol (ul)**	**Yield (ng)**	**Index1**	**Index1 Sequence**	**Index2**	**Index2 Sequence**
1	SO_10770_3	34.6	10	346	365	GAAGAGATGT	365	AGGAATATCG

Table 3: Barcode used for sequencing

Sample ID	Barcode name	Sequence
SO_10770_1	**NB85**	AACGGAGGAGTTAGTTGGATGATC
SO_10770_3	NB86	AGGTGATCCCAACAAGCGTAAGTA

Table-4 Susceptibility information

Antimicrobial	**MIC**	**Interpretation**
Ticarcillin/Clavulanic acid	>= 128	Resistant
Piperacillin/Tazobactam	>=128	Resistant
Ceftazidime	>=64	Resistant
Cefoperazone/Sulbactum	>=64	Resistant
Cefepime	>=64	Resistant
Doripenem	>=8	Resistant

Imipenem	>=16	Resistant
Meropenem	>=16	Resistant
Gentamicin	>=16	Resistant
Ciprofloxacin	>=4	Resistant
Levofloxacin	>=8	Resistant
Minocycline	>=16	Resistant
Tigecycline	>=2	Resistant
Colistin	>=0.5	Resistant
Trimethoprim/Sulfamethoxazole	>=320	Resistant

Table 5: Illumina read statistics

Sample Name	**SO_10770_3**
Raw Read Count	2817112
Sequencing Coverage (X)	211.28
Processed Read Count	2757479
% Reads Retained	97.88

Table 6: Nanopore read statistics

Sample Name	**SO_10770_3**	**SO_10770_3**
Mean read length	2071.3	1991.2
Mean read quality	12.1	12.5
Median read length	643	560
Median read quality	12.2	12.6
Number of reads	401126	400883
STDEV read length	4205.5	4206.2
Total bases	830841924	798256590
>Q7 Read Count	401126	400881
>Q10 ReadCount	353898	358990
Sequencing Coverage (X)	207.71	199.56

Table 7: Assembly statistics

Sample Name	**SO_10770_3**
Contigs Generated	3
Maximum Contig Length	4075173
Minimum Contig Length	2278
Average Contig Length	1362154.3
Median Contig Length	9012
Total Contigs Length	4086463
Total Number of Non-ATGC Characters	0
Percentage of Non-ATGC Characters	0
Contigs >=1Kbp	3
Contigs >=10Kbp	1
Contigs >=1Mbp	1
N50 value	4075173

Table 8: Novel Anti-microbial resistant Gene Family And mechanism of resistance in A baumannii strain SO_10770_3

AMR Gene Family	**Drug Class**	**Resistance Mechanism**
Resistance-nodulation-cell division (RND) antibiotic efflux pump	carbapenem; cephalosporin; diaminopyrimidine antibiotic; fluoroquinolone antibiotic; lincosamide antibiotic-macrolide antibiotic- penem, phenicol antibiotic-rifamycin antibiotic-tetracycline antibiotic	antibiotic efflux
Resistance-nodulation-cell division (RND) antibiotic efflux pump	fluoroquinolone antibiotic-tetracycline antibiotic	antibiotic efflux
Resistance-nodulation-cell division (RND) antibiotic efflux pump	Glycylcycline-tetracycline antibiotic	antibiotic efflux
Rifamycin-resistant beta-subunit of RNA polymerase (rpoB)	peptide antibiotic-rifamycin antibiotic	antibiotic target alteration in antibiotic target replacement
fluoroquinolone resistant gyrA	fluoroquinolone antibiotic-neomycin	antibiotic target alteration
Resistance-nodulation-cell division (RND) Antibiotic efflux pump	aminoglycoside antibiotic-fluoroquinolone antibiotic	antibiotic efflux
Fluoroquinolone resistant parC	fluoroquinolone antibiotic	antibiotic target alteration
ABC-F ATP-binding cassette ribosomal protection protein	lincosamide antibiotic-macrolide antibiotic-oxazolidinone antibiotic-phenicol antibiotic-pleuromutilin antibiotic-streptogramin antibiotic-tetracycline antibiotic	antibiotic target protection
Resistance-nodulation-cell division (RND) antibiotic efflux pump	aminoglycoside antibiotic-benzalkonium chloride; carbapenem -cephalosporin, Glycylcycline, penam, tetracycline antibiotic	antibiotic efflux
Resistance-nodulation-cell division (RND) antibiotic efflux pump	Glycylcycline-tetracycline antibiotic	antibiotic efflux
Multidrug and toxic compound extrusion (MATE) transporter	acridine dye-disinfecting agents and intercalating dyes-fluoroquinolone antibiotic-triclosan	antibiotic efflux
Resistance-nodulation-cell division (RND) antibiotic efflux pump	Carbapenem-cephalosporin, diaminopyrimidine antibiotic-fluoroquinolone antibiotic-lincosamide antibiotic-macrolide antibiotic-penem-phenicol antibiotic-rifamycin antibiotic-tetracycline antibiotic	antibiotic efflux
Resistance-nodulation-cell division (RND) antibiotic efflux pump	Carbapenem, cephalosporin, diaminopyrimidine antibiotic-fluoroquinolone antibiotic-lincosamide antibiotic-macrolide antibiotic-penem, phenicol antibiotic-rifamycin antibiotic-tetracycline antibiotic	antibiotic efflux
Major facilitator superfamily (MFS) antibiotic efflux pump	acridine dye- disinfecting agents and intercalating dyes-macrolide antibiotic	antibiotic efflux

Resistance-nodulation-cell division (RND) antibiotic efflux pump	fluoroquinolone antibiotic-tetracycline antibiotic	antibiotic efflux
major facilitator superfamily (MFS) antibiotic efflux pump	fosfomycin	antibiotic efflux
ADC beta-lactamase without carbapenemase activity	cephalosporin	antibiotic inactivation
major facilitator superfamily (MFS) antibiotic efflux pump	fluoroquinolone antibiotic	antibiotic efflux
ampC-type beta-lactamase	**Cephalosporin, penam**	**antibiotic inactivation**
Intrinsic peptide antibiotic resistant Lps B	**peptide antibiotic - Colistin**	**reduced permeability to antibiotic**
Resistance-nodulation-cell division (RND) antibiotic efflux pump	Carbapenem, cephalosporin, diaminopyrimidine antibiotic-fluoroquinolone antibiotic-lincosamide antibiotic-macrolide antibiotic-penem, phenicol antibiotic-rifamycin antibiotic-tetracycline antibiotic	antibiotic efflux
Resistance-nodulation-cell division (RND) antibiotic efflux pump	fluoroquinolone antibiotic-tetracycline antibiotic	antibiotic efflux
Major facilitator superfamily (MFS) antibiotic efflux pump	phenicol antibiotic	antibiotic efflux
Resistance-nodulation-cell division (RND) antibiotic efflux pump	fluoroquinolone antibiotic-tetracycline antibiotic	antibiotic efflux
Major facilitator superfamily (MFS) antibiotic efflux pump	phenicol antibiotic	antibiotic efflux
Outer Membrane Porin (Opr)	Carbapenem, cephalosporin, cephamycin, monobactam, penam.	reduced permeability to antibiotic resistance by absence
Acinetobacter mutant Lpx gene conferring resistance to colistin	**peptide antibiotic - Colistin**	**antibiotic target alteration**
PER beta-lactamase	Carbapenem, cephalosporin, monobactam, penam, penem	antibiotic inactivation
macrolide phosphotransferase (MPH)	macrolide antibiotic	antibiotic inactivation
elfamycin resistant EF-Tu	elfamycin antibiotic	antibiotic target alteration
APH(6)	aminoglycoside antibiotic	antibiotic inactivation
OXA beta-lactamase	Carbapenem, cephalosporin, penam	antibiotic inactivation
OXA beta-lactamase + NOVEL 230 OXA- Gene families Discovered	Carbapenem, cephalosporin, penam	antibiotic inactivation
sulfonamide resistant sul	sulfonamide antibiotic, sulfone antibiotic	antibiotic target replacement
OXA beta-lactamase	Carbapenem, cephalosporin, monobactam, penam	antibiotic inactivation
APH(3")	aminoglycoside antibiotic	antibiotic inactivation
OXA beta-lactamase	Carbapenem, cephalosporin, penam	antibiotic inactivation
PER beta-lactamase	Carbapenem, cephalosporin, monobactam, penam, penem	antibiotic inactivation
PER beta-lactamase	Carbapenem, cephalosporin, monobactam, penam, penem	antibiotic inactivation
Acinetobacter mutant Lpx gene conferring resistance to colistin	**Peptide antibiotic – Colistin**	antibiotic target alteration
elfamycin resistant EF-Tu	elfamycin antibiotic	antibiotic target alteration
16S rRNA methyltransferase (G1405)	aminoglycoside antibiotic	antibiotic target alteration
elfamycin resistant EF-Tu	elfamycin antibiotic	antibiotic target alteration
sulfonamide resistant sul	sulfonamide antibiotic-sulfone antibiotic	antibiotic target replacement
Major facilitator superfamily (MFS) antibiotic efflux pump	phenicol antibiotic	antibiotic efflux
Resistance-nodulation-cell division (RND) antibiotic efflux pump	Carbapenem, cephalosporin, diaminopyrimidine antibiotic-fluoroquinolone antibiotic-lincosamide antibiotic-macrolide antibiotic-penem, phenicol antibiotic-rifamycin antibiotic-tetracycline antibiotic	antibiotic efflux

Table :9 Novel virulence factors of A baumannii strain SO_10770_3 carried by Mobile genetical (MGE) elements and their Mechanism

Gene	Virulence	Annotation
ABZJ_01014	Receptor Protein	putative receptor protein, putative Heme acquisition system receptor [Heme utilization (CVF769)] [Acinetobacter baumannii MDR-ZJ06]
adeG	Drug Inactivation	Cation/multidrug efflux pump [AdeFGH efflux pump/transport autoinducer (CVF773)] [Acinetobacter baumannii BJAB0715]
adeG	Drug Inactivation	RND family efflux transporter [AdeFGH efflux pump/transport autoinducer (CVF773)] [Acinetobacter baumannii AB0057]
adeG	Drug Inactivation	cation/multidrug efflux pump [AdeFGH efflux pump (VF0504)] [Acinetobacter baumannii ACICU]
adeG	Drug Inactivation	multidrug ABC transporter [AdeFGH efflux pump/transport autoinducer (CVF773)] [Acinetobacter baumannii SDF]
adeG, adef	Drug Inactivation	RND family efflux transporter [AdeFGH efflux pump/transport autoinducer (CVF773)] [Acinetobacter baumannii AB0057] . Membrane transport fusion protein ADeFGH efflux pump autoinducer
pgaA	Biofilm production -Quorum Sensing	biofilm synthesis protein [PNAG (Polysaccharide poly-N-acetylglucosamine) (CVF772)] [Acinetobacter baumannii AYE]
bfms	Biofilm production- Quorum Sensing	Signal transduction histidine kinase [Two-component system (CVF778)] [Acinetobacter baumannii BJAB0715]
bfms	Biofilm production- Quorum Sensing	Two-component system sensor kinase protein [Two-component system (CVF778)] [Acinetobacter baumannii AB0057]
barA	Drug Inactivation	siderophore efflux system of the ABC superfamily [Acinetobactin (VF0467)] [Acinetobacter baumannii ACICU]
M3Q_281	Capsule Formation	tyrosine-protein kinase [Capsule (CVF775)] [Acinetobacter baumannii TYTH-1]
ABTJ_03743	Capsule Formation	phosphomannomutase [Capsule (CVF775)] [Acinetobacter baumannii MDR-TJ]
AB57_0115	Capsule Formation	phosphomannomutase [Capsule (CVF775)] [Acinetobacter baumannii MDR-TJ]
BJAB07104_00106	Capsule Formation	phosphomannomutase [Capsule (CVF775)] [Acinetobacter baumannii MDR-TJ]
BJAB0715_00115	Capsule	Phosphomannomutase [Capsule (CVF775)] [Acinetobacter baumannii BJAB0715]
manB	Capsule	bifunctional phosphomannomutase /phosphoglucomutans [Capsule (CVF775)] [Acinetobacter baumannii SDF]
Pgi, ABD1_00590 ABZJ_00088	Capsule	1.glucose-6-phosphate isomerase [Capsule (CVF775)] [Acinetobacter baumannii ATCC 17978] 2.protein WbjC [Capsule (CVF775)] [Acinetobacter baumannii MDR-ZJ06] 3. Capsular polysaccharide biosynthesis.
adeH	Drug Inactivation	NodT family efflux transporter outer membrane lipoprotein [AdeFGH efflux pump/transport autoinducer (CVF773)] [Acinetobacter baumannii TYTH-1]
lpxB	Lipid A Synthesis	Lipid A disaccharide synthetase [LPS (CVF774)] [Acinetobacter baumannii BJAB0715]
lpsB	Lipopolysaccaride	glycosyltransferase [LPS (CVF774)] [Acinetobacter baumannii D1279779]
lpxD		UDP-3-O-[3-hydroxymyristoyl] glucosamine N-acyltransferase [LPS (CVF774)] [Acinetobacter baumannii BJAB0715]
lpxM		lipid A biosynthesis lauroyl acyltransferase [LPS (CVF774)] [Acinetobacter baumannii ATCC 17978]
lpxL	Lipid A	Lauroyl/myristoyl acyltransferase [LPS (CVF774)] [Acinetobacter baumannii BJAB0715]
lpxL	Lipid A	htrB [LPS (CVF774)] [Acinetobacter baumannii 1656-2]
ompA	Cell Wall Synthesis	Outer membrane protein-related peptidoglycan-associated (lipo)protein [Outer membrane protein (CVF776)] [Acinetobacter baumannii BJAB0715]
ompA		outer membrane protein A precursor [Outer membrane protein (CVF776)] [Acinetobacter baumannii D1279779]
lpxC	Lipopolysaccaride	lpxC [LPS (CVF774)] [Acinetobacter baumannii 1656-2]
		UDP-3-O-[3-hydroxymyristoyl] N-acetylglucosamine deacetylase [LPS (CVF774)] [Acinetobacter baumannii SDF]
pilT	Pilin synthesis	twitching motility protein [Type IV pili biosynthesis (CVF518)] [Pseudomonas mendocina ymp]
		Pilus retraction protein PilT [Type IV pili biosynthesis (CVF518)] [Pseudomonas syringae pv. syringae B728a]
htpB		Hsp60, 60K heat shock protein HtpB [Hsp60 (CVF347)].
		60 kDa chaperonin (Protein Cpn60)(groEL protein)(Heat shock protein B). [Hsp60 (CVF347)] [Legionella pneumophila str. Lens]
		molecular chaperone GroEL [Hsp60 (CVF347)] [Legionella longbeachae NSW150]

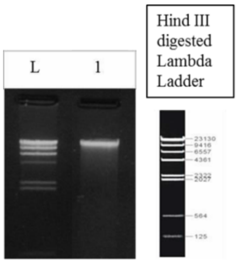

LANES	SAMPLES
L	Hind III digested Lambda Ladder
1	SO_10770_3

Figure1: Agarose gel electrophoresis of sample

Enzymatic fragmentation + End-repair + 3' adenylation (QIASeq FX DNA Library Kit)
↓
Adapter Ligation
↓
Library amplification and Indexing
↓
Library clean-up
↓
Quality check and Fragment size analysis

Figure 2: Work flow for QIA Seq FXDNA Library Preparation

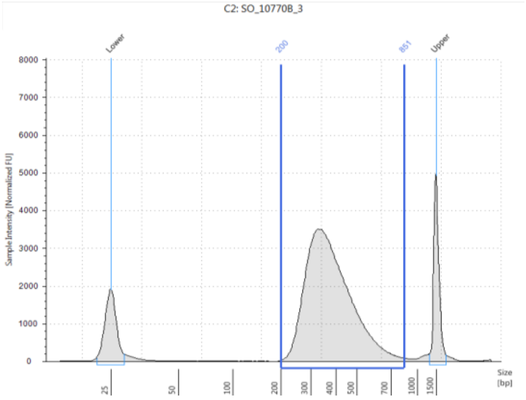

Figure 3: Tape Station Profile of SO_10770_3

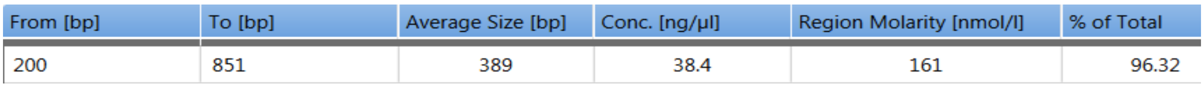

From [bp]	To [bp]	Average Size [bp]	Conc. [ng/µl]	Region Molarity [nmol/l]	% of Total
200	851	389	38.4	161	96.32

Figure 4: Overview of Nanopore Library Preparation

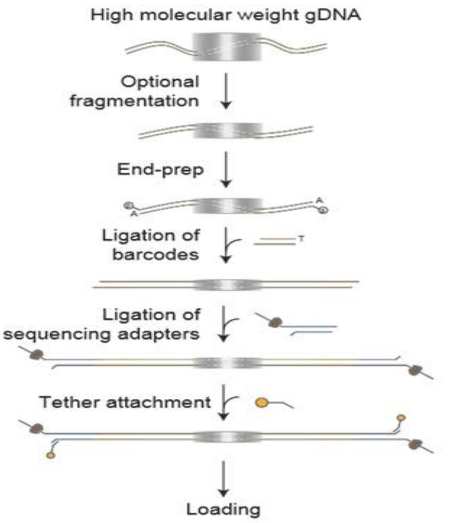

Figure 5: WGS bioinformatics work flow

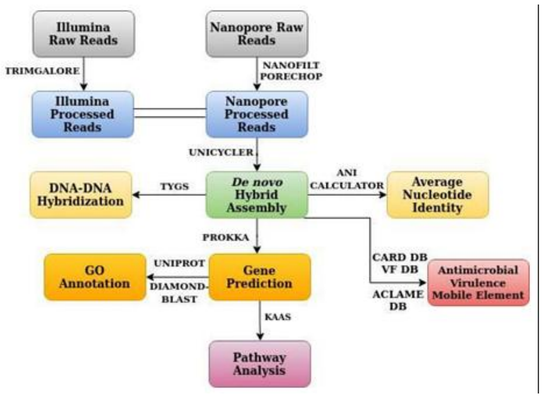

Figure 6a: NCBI NR blast result for contig1 (SO_10770_3)

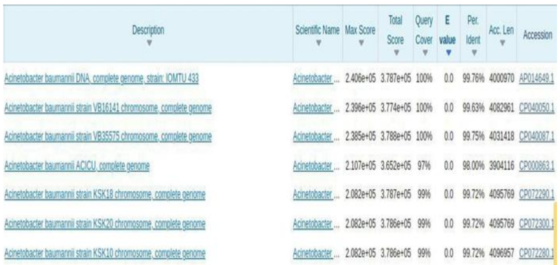

Description	Scientific Name	Max Score	Total Score	Query Cover	E value	Per. Ident	Acc. Len	Accession
Acinetobacter baumannii DNA, complete genome, strain: IOMTU 433	Acinetobacter ...	2.406e+05	3.787e+05	100%	0.0	99.76%	4000970	AP014649.1
Acinetobacter baumannii strain VB16141 chromosome, complete genome	Acinetobacter ...	2.396e+05	3.774e+05	100%	0.0	99.63%	4082961	CP040050.1
Acinetobacter baumannii strain VB35575 chromosome, complete genome	Acinetobacter ...	2.385e+05	3.788e+05	100%	0.0	99.75%	4031418	CP040087.1
Acinetobacter baumannii ACICU, complete genome	Acinetobacter ...	2.107e+05	3.652e+05	97%	0.0	98.00%	3904116	CP000863.1
Acinetobacter baumannii strain KSK18 chromosome, complete genome	Acinetobacter ...	2.082e+05	3.787e+05	99%	0.0	99.72%	4095769	CP072290.1
Acinetobacter baumannii strain KSK20 chromosome, complete genome	Acinetobacter ...	2.082e+05	3.786e+05	99%	0.0	99.72%	4095769	CP072300.1
Acinetobacter baumannii strain KSK10 chromosome, complete genome	Acinetobacter ...	2.082e+05	3.786e+05	99%	0.0	99.72%	4096957	CP072280.1

Figure 6b: NCBI NR blast result for contig2 (SO_10770_3)

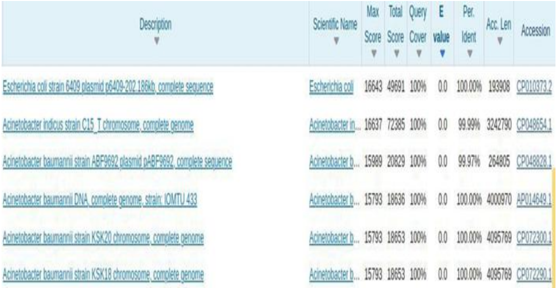

Description	Scientific Name	Max Score	Total Score	Query Cover	E value	Per. Ident	Acc. Len	Accession
Escherichia coli strain 6409 plasmid p6409-202.186kb, complete sequence	Escherichia coli	16643	49691	100%	0.0	100.00%	193908	CP010373.2
Acinetobacter indicus strain C15_T chromosome, complete genome	Acinetobacter in...	16637	72385	100%	0.0	99.99%	3242790	CP048654.1
Acinetobacter baumannii strain ABF9692 plasmid pABF9692, complete sequence	Acinetobacter b...	15989	20829	100%	0.0	99.97%	264805	CP048828.1
Acinetobacter baumannii DNA, complete genome, strain: IOMTU 433	Acinetobacter b...	15793	18636	100%	0.0	100.00%	4000970	AP014649.1
Acinetobacter baumannii strain KSK20 chromosome, complete genome	Acinetobacter b...	15793	18653	100%	0.0	100.00%	4095769	CP072300.1
Acinetobacter baumannii strain KSK18 chromosome, complete genome	Acinetobacter b...	15793	18653	100%	0.0	100.00%	4095769	CP072290.1

Figure 6c: NCBI NR blast result for contig3 (SO_10770_3)

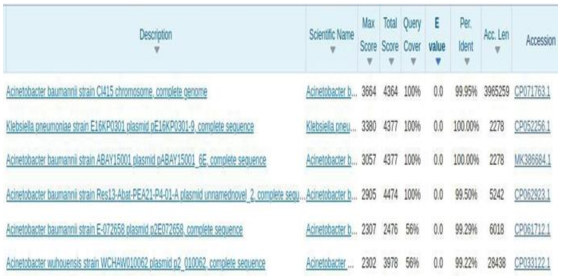

Description	Scientific Name	Max Score	Total Score	Query Cover	E value	Per. Ident	Acc. Len	Accession
Acinetobacter baumannii strain CI415 chromosome, complete genome	Acinetobacter b...	3664	4364	100%	0.0	99.95%	3965259	CP071763.1
Klebsiella pneumoniae strain E16KP0301 plasmid pE16KP0301-9, complete sequence	Klebsiella pneu...	3380	4377	100%	0.0	100.00%	2278	CP052256.1
Acinetobacter baumannii strain ABAY15001 plasmid pABAY15001_6E, complete sequence	Acinetobacter b...	3057	4377	100%	0.0	100.00%	2278	MK386684.1
Acinetobacter baumannii strain Res13-Abat-PEA21-P4-01-A plasmid unnamednovel_2, complete sequ...	Acinetobacter b...	2905	4474	100%	0.0	99.50%	5242	CP062923.1
Acinetobacter baumannii strain E-072658 plasmid p2E072658, complete sequence	Acinetobacter b...	2307	2476	56%	0.0	99.29%	6018	CP061712.1
Acinetobacter wuhouensis strain WCHAW010062 plasmid p2_010062, complete sequence	Acinetobacter ...	2302	3978	56%	0.0	99.22%	28438	CP033122.1

Figure 7: GO annotation image for sample SO_10770_3

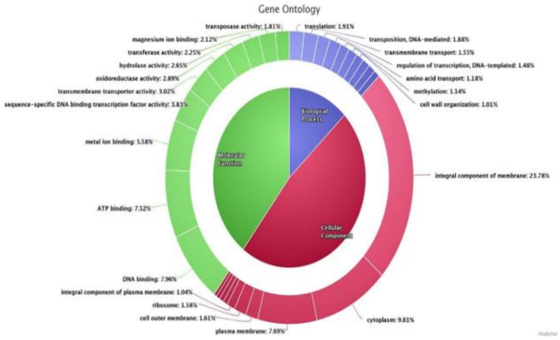

Figure 8: Top 10 pathway functions for sample SO_10770_3

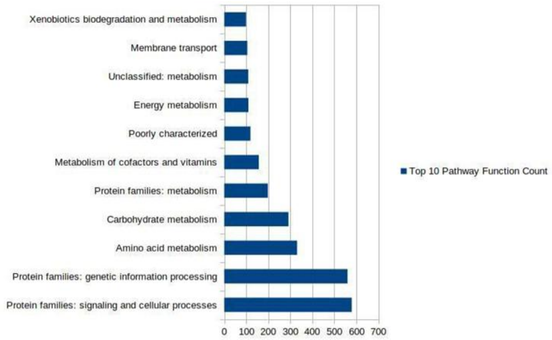

Figure 9: Whole genome level phylogenetic tree for sample SO_10770_3

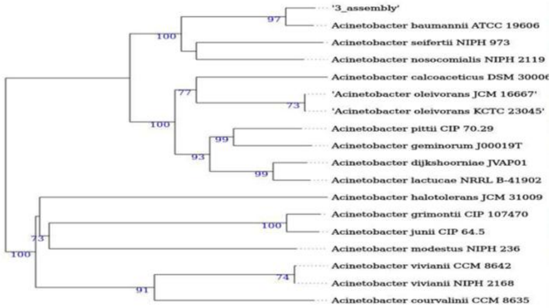

Figure 10: ANI plot between sample SO_10770_3 and reference strain

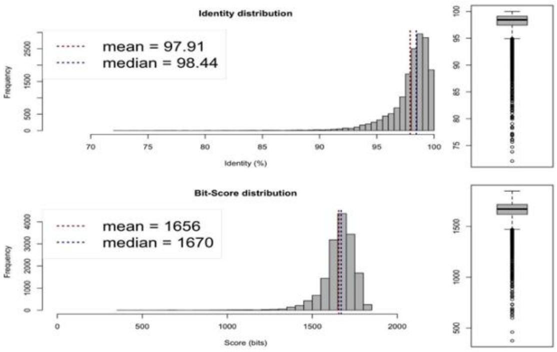

Figure 11: BRIG Circular genome comparison image of sample SO_10770_3 plotted with Anti Microbial Resistant (AMR) Genes and reference Acinetobacter baumannii ATCC19606 strain

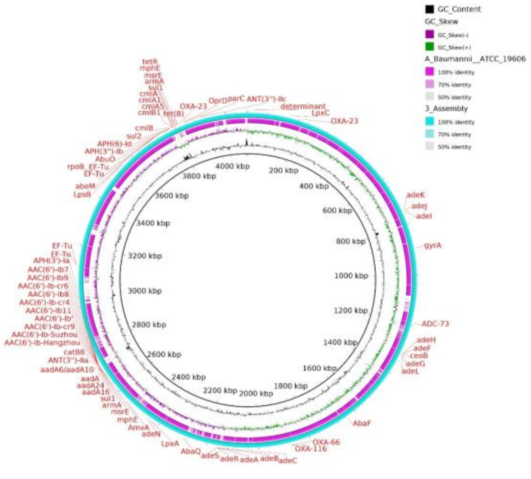

Figure :12 Virulence factor Genes plotted on BRIG Diagram for SO_10770_3 Strain and Reference Acinetobacter baumannii stain ATCC 19606